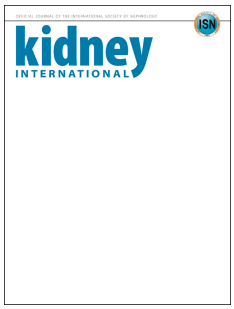

The sodium/proton exchanger NHA2 regulates blood pressure through a WNK4-NCC dependent pathway in the kidney.

Manuel A. Anderegg, Giuseppe Albano, Daniela Hanke, Christine Deisl, Dominik E. Uehlinger, Simone Brandt, Rajesh Bhardwaj, Matthias A. Hediger, Daniel G. Fuster

PII: S0085-2538(20)31066-8

DOI: https://doi.org/10.1016/j.kint.2020.08.023

Reference: KINT 2292

To appear in: *Kidney International*

Received Date: 30 March 2020

Revised Date: 13 August 2020

Accepted Date: 26 August 2020

Please cite this article as: Anderegg MA, Albano G, Hanke D, Deisl C, Uehlinger DE, Brandt S, Bhardwaj R, Hediger MA, Fuster DG, The sodium/proton exchanger NHA2 regulates blood pressure through a WNK4-NCC dependent pathway in the kidney., *Kidney International* (2020), doi: https://doi.org/10.1016/j.kint.2020.08.023.

The sodium/proton exchanger NHA2 regulates blood pressure through a WNK4-NCC dependent pathway in the kidney.

NHA2 KO
NCC/NHA2 double KO

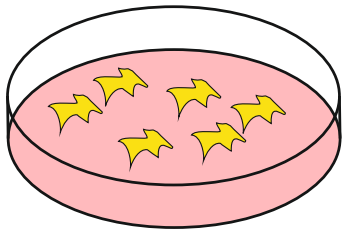

mpkDCT4
HEK293

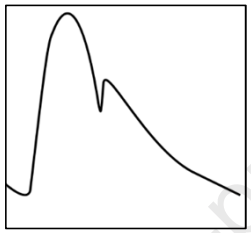

Loss of NHA2 - in vivo

- ↓ Blood pressure
- ↓ Urine calcium
- ↓ Response to HCT

Loss of NHA2 - in vitro

- ↓ pNCC
- ↓ pSPAK
- ↓ WNK4

CONCLUSION:

Our study reveals NHA2 as a novel regulator of the WNK4-NCC pathway in the distal convoluted tubule.

kidney INTERNATIONAL
OFFICIAL JOURNAL OF THE INTERNATIONAL SOCIETY OF NEPHROLOGY

Anderegg et al., 2020

[QUERY TO AUTHOR: title and abstract rewritten by Editorial Office – not subject to change]

The sodium/proton exchanger NHA2 regulates blood pressure through a WNK4-NCC dependent pathway in the kidney.

Manuel A. Anderegg[1,2,3], Giuseppe Albano[1,2,3], Daniela Hanke[1,2,3], Christine Deisl[1,2,3], Dominik E. Uehlinger[1], Simone Brandt[4], Rajesh Bhardwaj[1,2,3], Matthias A. Hediger[1,2,3], Daniel G. Fuster[1,2,3,5 *]

[1]Department of Nephrology and Hypertension, Inselspital, Bern University Hospital, University of Bern, Switzerland, [2]Swiss National Centre of Competence in Research (NCCR) TransCure, University of Bern, Switzerland, [3]Department of Biomedical Research, University of Bern, Switzerland, [4]Department of Pathology and Molecular Pathology, University Hospital Zürich, University of Zürich, Switzerland, [5]Swiss National Centre of Competence in Research (NCCR) Kidney.CH, University of Zürich, Switzerland

[*]Correspondence:

Prof. Dr. med. Daniel G. Fuster

Department of Nephrology and Hypertension, Inselspital, Bern University Hospital, University of Bern, Freiburgstrasse 15, 3010 Bern, Switzerland

Email: Daniel.Fuster@insel.ch

Phone: ++41 (0)31 632 31 44

Fax: ++41 (0)31 632 97 34

Running title: NHA2 regulates blood pressure

Word count: 4372

ABSTRACT

NHA2 is a sodium/proton exchanger associated with arterial hypertension in humans, but the role of NHA2 in kidney function and blood pressure homeostasis is currently unknown. Here we show that NHA2 localizes almost exclusively to distal convoluted tubules in the kidney. NHA2 knock-out mice displayed reduced blood pressure, normocalcemic hypocalciuria and an attenuated response to the thiazide diuretic hydrochlorothiazide. Phosphorylation of the thiazide-sensitive sodium/chloride cotransporter NCC and its upstream activating kinase Ste20/SPS1-related proline/alanine rich kinase (SPAK), as well as the abundance of with no lysine kinase 4 (WNK4), were significantly reduced in the kidneys of NHA2 knock-out mice. *In vitro* experiments recapitulated these findings and revealed increased WNK4 ubiquitylation and enhanced proteasomal WNK4 degradation upon loss of NHA2. The effect of NHA2 on WNK4 stability was dependent from the ubiquitylation pathway protein Kelch-like 3 (KLHL3) . More specifically, loss of NHA2 selectively attenuated KLHL3 phosphorylation and blunted protein kinase A- and protein kinase C-mediated decrease of WNK4 degradation. Phenotype analysis of NHA2/NCC double knock-out mice supported the notion that NHA2 affects blood pressure homeostasis by a kidney-specific and NCC-dependent mechanism. Thus, our data show that NHA2 as a critical component of the WNK4-NCC pathway and is a novel regulator of blood pressure homeostasis in the kidney.

Keywords: Sodium/hydrogen exchanger, blood pressure, urine calcium, thiazide, ubiquitylation, WNK4, KLHL3, NCC, NHA2

TRANSLATIONAL STATEENT

Arterial hypertension affects millions of patients worldwide and is a significant cause of excess morbidity and mortality. In most cases, the underlying mechanisms of increased blood pressure remain obscure, broadly designated as “essential hypertension”. A better understanding of the molecular pathogenesis of arterial hypertension may foster the development of novel diagnostic, preventive and therapeutic strategies. Our study reveals that the sodium/hydrogen exchanger NHA2 localizes to distal convoluted tubules in the kidney and is critical for electrolyte and blood pressure homeostasis in mice. Future studies are needed to explore the role of NHA2 in kidney function and blood pressure homeostasis in humans.

INTRODUCTION

Na^+/H^+ exchangers (NHEs; *SLC9* gene family) exchange monovalent cations like Na^+, Li^+ or K^+ with protons across lipid bilayers and are present in prokaryotes and eukaryotes [1]. In mammals, 12 NHE isoforms are known thus far, grouped in three subfamilies SLC9A, SLC9B and SLC9C, respectively [2]. NHA1 and NHA2 (also known as SLC9B1 and SLC9B2) constitute the SLC9B family, but their function remains poorly defined. Based on chromosomal localization, transport characteristics and inhibitor sensitivity, NHA2 was proposed to be the long sought mediator of Na^+/Li^+ counter-transport (SLC) [3]. SLC activity is a highly heritable trait, associated with abnormalities in Na^+ homeostasis, diabetes mellitus and arterial hypertension in humans [4-9]. We previously demonstrated that NHA2 resides in endosomes of β-cells and is critical for insulin secretion [10, 11]. In support of this finding, a single-nucleotide polymorphism in the *NHA2* gene was recently discovered in a genome-wide association study as a new locus associated with type 2 diabetes in humans [12]. In the rodent kidney, NHA2 was previously detected in the distal nephron, including the distal convoluted tubules (DCT), but its quantitative expression pattern along the nephron remains unknown [13, 14]. In addition, the role of NHA2 in kidney function and blood pressure homeostasis has not been studied and thus remains elusive.

DCT cells express the apical thiazide-sensitive Na^+ / Cl^- cotransporter NCC (also known as SLC12A3). NCC activity is regulated by an intricate kinase network with the serine-threonine with-no-lysine kinase 4 (WNK4) at its core [15]. Once activated, WNK4 phosphorylates the Ste20/SPS1-related proline/alanine-rich kinase (SPAK), which in turn phosphorylates and activates NCC. WNK4 abundance and activity are tightly controlled by posttranslational modifications. An E3-RING ubiquitin ligase complex that includes the two regulatory proteins Cullin 3 (CUL3) and Kelch-like 3 (KLHL3), ubiquitylates WNK4 and thereby induces its proteasomal degradation. Protein kinase C (PKC) and protein kinase A (PKA), activated by angiotensin II and vasopressin, respectively, directly phosphorylate and activate

WNK4 [16]. In addition, PKC and PKA were also shown to phosphorylate KLHL3, which leads to disruption of the KLHL3-WNK4 interaction and hence prevents WNK4 ubiquitylation [17, 18].

The DCT is paramount for blood pressure homeostasis in mammals. Biallelic loss-of-function mutations or deletions of *NCC* result in Gitelman's syndrome, characterized by hypotension, hypokalemia, metabolic alkalosis and hypocalciuria [19, 20]. In contrast, dominant mutations in *WNK1*, *WNK4*, *CUL3* or *KLHL3* cause the mirror phenotype, pseudohypoaldosteronism type II (PHA II, also known as Gordon's syndrome), characterized by hypertension, hyperkalemia, metabolic acidosis and hypercalciuria [21-23]. Clinical PHA II features are corrected with pharmacological blockade of NCC by thiazide diuretics, supporting the notion that increased NCC activity is the hallmark of PHA II [24].

The aim of the present study was to explore the role of NHA2 in the kidney. Our results demonstrate that NHA2 has predominant DCT expression and that genetic disruption of NHA2 in mice results in a Gitelman-like phenotype. *In vitro* and *in vivo* studies, including phenotypic assessment of NHA2 / NCC double KO mice, indicate that NHA2 controls WNK4 abundance and thereby NCC activity in a cell-autonomous manner in the kidney. Thus, our study reveals NHA2 as a novel regulator of electrolyte and blood pressure homeostasis in the mammalian kidney.

RESULTS

The DCT is the main site of NHA2 expression in the kidney

To examine NHA2 expression in the murine kidney, we first performed confocal imaging of kidney cryosections. As shown in Fig. 1A, NHA2 expression exhibits a prominent tubular expression pattern in wild-type (WT) mouse kidneys, while no signal was detected with the secondary antibody only control or in kidneys of NHA2 knock-out (NHA2 KO) mice stained with the NHA2 antibody [11]. To further delineate the tubular expression pattern, we conducted confocal imaging studies in serial cryosections probed for NHA2 and well-established markers of the distal nephron in the mouse [25]. NHA2 co-localized with parvalbumin (a marker of DCT 1) but also with TRPV5, NCX1 and Calbindin D $_{28k}$ (markers of DCT2 and CNT, respectively) (Fig. 1B and Suppl. Fig. 1). Quantitative real-time PCR analysis of microdissected murine kidney tubules confirmed the expression pattern observed by confocal imaging (Fig. 1 C and Suppl. Fig. 2). NHA2 mRNA expression was primarily confined to DCT with significantly lower expression in connecting tubules (CNT) and cortical collecting ducts (CCD). In the latter, NHA2 was observed in both principal and intercalated cells (Suppl. Fig. 1). Of note, however, no expression of NHA2 was observed in segments proximal to the DCT.

NHA2 KO mice display normocalcemic hypocalciuria, hyperaldosteronism and reduced blood pressure

In a next step, we measured blood (Table 1) and urinary (Table 2) parameters in 3 months old WT and NHA2 KO mice. Twenty-four-hour urines were collected in metabolic cages after an adaptation phase of 2 days. NHA2 KO mice exhibited no significant differences in serum electrolytes, renal function parameters, parathyroid hormone (PTH) and 1,25-OH Vitamin D. Urinary Ca^{++} excretion was significantly reduced in NHA2 KO mice, but all other parameters were similar in WT and NHA2 KO mice. In addition, we observed increased urinary

aldosterone in NHA2 KO mice, whereas excretion of glucocorticoids (corticosterone) and catecholamines (adrenaline and noradrenaline) were unaltered.

Thus, NHA2 KO mice display normocalcemic hypocalciuria and hyperaldosteronism, hallmarks of DCT dysfunction, as seen in Gitelman's syndrome or upon treatment with thiazides. To further delineate the phenotype, we next performed blood pressure measurements by telemetry [26]. Blood pressure was recorded for 3 consecutive days under low (<0.03%), normal (0.2 %) and high Na^+ (8 %) diets in steady state condition after an equilibration phase of 1 week each with the respective diet. As shown in Fig. 2 and Suppl. Fig. 3A, blood pressure was significantly lower in NHA2 KO mice with all diets, but the difference between the two groups of mice became more pronounced with increasing Na^+ content of the diet.

Reduced WNK4 abundance and NCC phosphorylation in kidneys of NHA2 KO mice

Phenotype analysis of NHA2 KO mice suggests DCT dysfunction upon loss of NHA2. To further substantiate these findings, we assessed expression of NCC and of upstream kinases SPAK and WNK in kidneys of WT and NHA2 KO mice. As shown in Figs. 3A and B, loss of NHA2 was associated with a reduction of phosphorylated NCC and SPAK as well as reduced abundance of WNK4, whereas expression of KLHL3 and CUL3 was unchanged. Total abundance of SPAK was unaltered, but we observed a decrease of full length and an increase of the inhibitory kidney-specific SPAK isoform (KS-SPAK) in NHA2 KO kidneys [27]. WNK4 transcript was similar in WT and NHA2 KO mice, suggesting a posttranslational mechanism as cause for the observed reduction of WNK4 protein expression upon loss of NHA2 (Suppl. Fig. 4). Transcript levels of typical DCT markers (NCC, parvalbumin, TRPM6, TRPV5, NCX1) were unaltered in NHA2 KO kidneys, but NHA2 KO mice exhibited higher renin expression compared to WT mice (Suppl. Fig. 4).

Previous studies demonstrated that NCC phosphorylation at threonine residues 53 and 58 in mice (equivalent to threonine 55 and 60 in human NCC) is associated with increased NCC transport activity [28-31]. To study NCC activity *in vivo*, we examined the sensitivity of WT and NHA2 KO mice to 50 mg/kg ip. hydrochlorothiazide (HCTZ). As shown in Fig. 3C and D, the natriuretic and hypocalciuric effect of HCTZ was greatly attenuated in NHA2 KO mice, compatible with reduced NCC activity.

In a next series of experiments, we investigated adaptive changes in NHA2 KO kidneys. In tubular segments proximal to the DCT - which all lack NHA2 (Fig. 1) - we observed evidence of increased activation of Na^+ transporters in kidneys of NHA2 KO mice, including increased phosphorylation of the Na^+ / K^+ / 2 Cl^- cotransporter NKCC2 and reduced phosphorylation of NHE3 at position S552 (Suppl. Figs. 5A-D) [32-34]. No adaptive changes were observed in segments distal to the DCT, expression of α-ENaC (both cleaved and uncleaved), β-ENaC, Pendrin and AE1 were not different between the two groups of mice.

Knock-out of NCC abolishes the effect of NHA2 deletion

To substantiate the claim that the kidney phenotype observed in NHA2 KO mice is due to reduced NCC activity, we next studied NCC and NCC/NHA2 double KO mice [35, 36]. Blood pressure measured by telemetry was lower in NCC and NCC/NHA2 double KO mice compared to WT or NHA2 KO mice (Suppl. Figs. 3, 6), but there was no difference in blood pressure between NCC and NCC/NHA2 double KO mice (Fig. 4A and Suppl. Fig. 3B). Similarly, calciuria was significantly reduced in NCC KO mice compared to WT or NHA2 KO mice, but the additional deletion of NHA2 did not further reduce calciuria (Fig. 4B). Thus, together with the fact that NCC is exclusively expressed in the kidney [37], these experiments support the notion that NHA2 affects blood pressure homeostasis via an intrarenal, NCC-dependent mechanism.

NHA2 regulates WNK-NCC axis in a cell autonomous manner

We previously demonstrated that NHA2 plays an important role in secretagogue-mediated insulin secretion in pancreatic β–cells [10, 11]. Three months old NHA2 KO mice fed a regular chow, as employed in the current study, have similar blood glucose and insulin levels in fasting and fed state compared to WT mice [10, 11]. Supraphysiological glucose challenges are necessary to unmask the insulin secretion deficit *in vivo*. Nevertheless, the observation of DCT dysfunction in global NHA2 KO mice may be secondary to systemic changes upon loss of NHA2. To explore this further, we first assessed phosphorylation of insulin receptor and AKT in kidneys of WT and NHA2 KO mice. As shown in Suppl. Figs. 5E, F, no differences were observed between the two groups of mice. Similarly, phosphorylation of serum- and glucocorticoid-inducible kinase 1 (SGK1), a kinase expressed in kidney tubules and phosphorylated by insulin and other growth factors, was unaltered in kidneys of NHA2 KO mice.

In a next step, we studied the impact of NHA2 depletion on a cellular level *in vitro*, using mpkDCT$_4$ cells, a well-characterized murine DCT cell line that expresses NCC (Suppl. Fig. 7) [29, 38-41]. SiRNA-mediated knock-down of NHA2 in mpkDCT$_4$ cells caused a significant reduction in endogenous WNK4 expression (Figs. 5A, B) that was associated with an attenuation of low Cl^- - or angiotensin II (ATII)-induced NCC phosphorylation, whereas total abundance of NCC remained unchanged (Figs. 5C-F). Together, these results indicate that NHA2 affects the WNK-NCC axis directly in a cell-autonomous way.

Loss of NHA2 enhances KLHL3-dependent ubiquitylation of WNK4

Given the known posttranslational regulation of WNK4, we next assessed WNK4 ubiquitylation in HEK293 cells. Knock-down of endogenous NHA2 in WNK4 transfected

HEK293 cells caused a significant reduction of WNK4 abundance, as observed in mpkDCT$_4$ cells (Figs. 6A, B, Suppl. Fig. 7). Reduced WNK4 abundance was paralleled by an increase in WNK4 ubiquitylation (Figs. 6A, B) and treatment with the proteasomal inhibitor Mg132 rescued WNK4 expression (Figs. 6C, D). To ascertain that increased WNK4 ubiquitylation was mediated by the E3 ligase KLHL3 and not by a KLHL3-independent pathway, we performed additional experiments with point mutants in the acidic box domain of WNK4 (E562K and Q565E) that disrupt WNK4-KLHL3 interaction and are associated with a PHA II phenotype in humans [22, 42]. As shown in Figs. 6E, F, expression levels of acidic box WNK4 mutants were unaffected by NHA2 depletion, indicating that NHA2 affects WNK4 abundance in a KLHL3-dependent manner.

PKA and PKC, activated by vasopressin and AT II, respectively, increase WNK4 levels by promoting KLHL3 phosphorylation and thereby disrupting WNK4-KLHL3 interaction [17, 18]. In cells with NHA2 depletion, we observed impaired PKC-mediated KLHL3 phosphorylation induced by PKC activator 12-O-tetradecanoylphorbol-13-acetate (TPA), whereas total abundance of KLHL3 was unchanged (Figs. 7A, B). The PKC inhibitor BIM was used as negative control alone or in combination with TPA. Knock-down of NHA2 did not affect levels of active, phosphorylated PKA or PKC isoforms responsible for KLHL3 phosphorylation nor the abundance of the phosphatase calcineurin, recently shown to be involved in KLHL3 dephosphorylation (Suppl. Fig. 8) [17, 18, 43]. In a next series of experiments, we directly stimulated PKA by forskolin (FK) and PKC by TPA. Both TPA (Figs. 7C, D) and FK (Figs. 7E, F) increased WNK4 expression in cells treated with control siRNA but not in cells with NHA2 depletion. Activation of PKA and PKC by FK and TPA, respectively, assessed by quantifying PKA and PKC phosphosubstrates with phosphospecific antibodies, were not affected upon knock-down of NHA2 (Figs. 7G-J). Together, these results indicate an impairment of KLHL3 phosphorylation as the underlying mechanisms of reduced WNK4 stability upon loss of NHA2.

NHA2 localizes to endosomes but does not co-localize or directly interact with WNK4 or KLHL3

We previously observed colocalization of NHA2 with markers of the endocytic pathway in pancreatic β-cells and osteoclasts [11, 44]. To assess the subcellular localization of NHA2 in DCT cells, we performed sucrose gradient subcellular fractionation studies with mpkDCT$_4$ cells (Suppl. Fig. 9). Equilibrium density centrifugation of mpkDCT$_4$ homogenates in linear sucrose gradients indicated that endogenous NHA2 was present in the same fractions as the transferrin receptor (TfR), a marker of recycling endosomes, but was absent in plasma membrane fractions (markers: NHE1 and NCC). However, we observed partial colocalization of NHA2 with WNK4, CUL3 and KLHL3. We next quantified endosomal and cytosolic pH in mpkDCT$_4$ and HEK293 cells treated with control or NHA2 siRNA or in HEK293 cells with NHA2 overexpression (Suppl. Fig. 10). Results obtained indicate that NHA2 does not influence endosomal or cytoplasmic pH in these cell lines. Given the known association of intracellular calcium with calcineurin activity and hence KLHL3 phosphorylation [43], we then determined intracellular calcium levels, store-operated calcium entry and membrane potential HEK293 cells treated with control or NHA2 siRNA (Suppl. Figs. 11, 12). These results revealed no differences between cells with and without NHA2 depletion. Thus, the exact molecular mechanism of how loss of NHA2 augments KLHL3-dependent WNK4 degradation remains enigmatic at the moment.

In summary, our data demonstrate that NHA2 is expressed in DCT cells of the kidney and loss of NHA2 causes a Gitelman-like phenotype in mice. Complementary *in vitro* and *in vivo* studies reveal the sodium/hydrogen exchanger NHA2 as a critical component of the WNK4-NCC pathway and hence as an important novel regulator of blood pressure homeostasis.

DISCUSSION

Our results demonstrate that NHA2 is critical for the maintenance of WNK4 levels and thus ultimately NCC activity in the DCT cell. Loss of NHA2 causes decreased KLHL3 phosphorylation and therey increased proteasomal WNK4 degradation. Enhanced WNK4 degradation is resistant to direct, receptor-independent PKA or PKC activation, indicating that the defect is at the post-receptor level i.e. not due to reduced activation of angiotensin or vasopressin receptors. Although we did not have kidney-specific NHA2 KO mice available for study, *in vitro* experiments with mpkDCT$_4$ and HEK293 cells suggest that NHA2 regulates WNK4 abundance by a cell autonomous rather than via an indirect, systemic way. This notion is corroborated by the observation that insulin receptor and AKT phosphorylation levels were equal in kidneys of WT and NHA2 KO mice. Phenotype analysis of NCC/NHA2 double KO mice furthermore indicate that NHA2 effects on electrolyte and blood pressure homeostasis are NCC- and hence kidney-dependent.

Blood pressure differences between WT and NHA2 KO mice become more pronounced with increased sodium intake. This is an unexpected finding and different from what would be expected in mice with a reduction or loss of NCC expression [35]. We do not have a definitive explanation for our observations, but speculate that the sodium-dependent regulation of NHA2 expression in the kidney may play a role. As recently shown, dietary sodium intake is a strong regulator of NHA2 expression in the kidney [14]. Compared to standard chow, a high sodium diet caused a ~5-fold upregulation of NHA2 transcript and protein in the kidney. Hence, it is to be expected that NHA2-mediated effects in the kidney (and as such the phenotypic difference between WT and NHA2 KO mice) become more pronounced with increasing dietary sodium intake. Additional studies are needed to test this hypothesis.

Our mRNA expression data in microdissected tubules revealed low levels of NHA2 mRNA in CNT and CCD, respectively. Although we failed to observe significant alterations in key

transport systems in CNT and CCD in NHA2 KO kidneys on mRNA or protein level, it is possible that NHA2 also influences tubular transport in these two segments. Our results obtained with NHA2 KO, NCC KO and NCC/NHA2 double KO mice, however, clearly indicate that NCC is the key mediator of NHA2 effects in the kidney.

We detected increased NKCC2 and decreased NHE3 phosphorylation, compatible with both increased NKCC2 and NHE3 activity, in kidneys of NHA2 KO mice. Given the lack of NHA2 expression in segments proximal to the DCT, we interpret these findings as secondary due to extracellular volume contraction, as evidenced by reduced blood pressure, increased urinary aldosterone excretion and renal renin expression in NHA2 KO mice [45-47]. Hypocalciuria in NHA2 KO mice is likely a consequence of volume contraction with augmented transcellular Na^+ and hence paracellular Ca^{++} reabsorption in segments proximal to the DCT, including the proximal tubule and TALH [48]. This notion is supported by the fact that we did not observe alterations in other mineral metabolism parameters in NHA2 KO mice and that selective loss (Gitelman's syndrome) or inhibition (thiazides) of NCC are also associated with hypocalciuria. However, a direct increase of Ca^{++} reabsorption at the level of the DCT in NHA2 KO mice remains a possibility that we cannot rule out at the moment.

How NHA2 ultimately regulates KLHL3-dependent WNK4 at a molecular level remains an unresolved issue. Confocal immunofluorescence staining of kidney cryosections displays apical / subapical staining of NHA2. Sucrose gradient centrifugation analysis of endogenous NHA2 in mpkDCT$_4$ cells support our previous findings in other cell lines and indicate that NHA2 is not present at the plasma membrane, but localizes to endosomes [11]. While depletion of NHA2 in both HEK293 and mpkDCT$_4$ cells reproduces changes observed in kidneys of NHA2 KO mice, it had no effect on endosomal pH. Similarly, we failed to detect a physical interaction of NHA2 with WNK4, KLHL3 or CUL3. Based on the sequence similarity with other mammalian and prokaryotic NHEs, NHA2 was proposed

to be a cation/proton exchanger. NHA2-mediated Na^+ and Li^+/H^+ exchange have initially been inferred from functional complementation studies in yeast [3, 13] but subsequently confirmed with purified human NHA2 in proteoliposomes [49]. In the latter study, however, not full length, but a shorter NHA2 transcript (isoform 2) lacking an exon encompassing the first transmembrane domain was studied. Interestingly, Chintapalli *et al.* recently suggested that the *D. melanogaster* orthologue of human NHA2 is in fact not a Na^+/H^+ exchanger, but a H^+/Cl^- co-transporter [50]. Our data suggest that NHA2 is not involved in endosomal pH homeostasis. In analogy to what has been proposed for the endosomal $2Cl^-/H^+$ exchanger CLC-5, NHA2 may participate in endosomal ion but not pH homeostasis or alternatively may be executing ion transport-independent functions in the endosome [51]. Clearly, more detailed information on NHA2 ion transport properties are needed to help further dissecting the role of NHA2 in the DCT at a molecular level.

MATERIALS AND METHODS

Unless specified otherwise, all chemicals and reagents were obtained from Sigma-Aldrich (St. Louis, MO, USA).

Plasmids

WNK4 constructs were a generous gift of S. Uchida, Tokyo Medical and Dental University, Japan, and reported previously [52, 53]. CUL3-FLAG and KLHL3-GFP was provided by the MRC phosphorylation Unit, University of Dundee, UK. Octameric, N-terminally tagged HA-ubiquitin was a gift of M. Treier and described in detail [54].

Cell culture and transfection

All cell lines used for experiments were tested mycoplasma free. Cells were grown in a humidified 95/5% air/CO2-atmosphere incubator at 37 °C. MpkDCT4 cells were cultured as described previously [39, 55-57]. Transient transfection was performed using cationic liposome (RNAimax, Life Technologies) followed by incubation for 48 h. The two siRNAs targeting murine NHA2 [58] and the control siRNA [59] were previously reported and validated. MpkDCT4 cells were stimulated with either control basic or hypotonic low-chloride medium, or DMEM without additives containing 10^{-6}M Angiotensin II, for 30 or 60 minutes, respectively. Cells were lysed in 0.3 ml of ice-cold lysis buffer/well, lysates were clarified by centrifugation at 4°C for 20 minutes at 20,000 x *g* and the supernatants were frozen or protein concentration was adjusted and samples were mixed with 4x Laemmli buffer. Lysis buffer contained 50 mM Tris/HCl, pH 7.5, 1 mM EGTA, 1 mM EDTA, 50 mM sodium fluoride, 5 mM sodium pyrophosphate, 1 mM sodium orthovanadate, 1% (w/v) NP-40, 0.27 M sucrose, 0.1% (v/v) 2-mercaptoethanol and 1x protease inhibitors [29]. Basic buffer contained 135 mM NaCl, 5 mM KCl, 0.5 mM $CaCl_2$, 0.5 mM MgCl2, 0.5 mM Na_2HPO_4, 0.5 mM Na_2SO_4 and 15 mM HEPES. Hypotonic low-chloride buffer contained 67.5 mM Na gluconate, 2.5 mM K

gluconate, 0.25 mM $CaCl_2$, 0.25 mM $MgCl_2$, 0.5 mM Na_2HPO_4, 0.5 mM Na_2SO_4 and 7.5 mM HEPES. HEK293 were obtained from ATCC and cultured in DMEM (GIBCO) supplemented with 10% (vol/vol) heat-inactivated FBS, 5mM Hepes, Na-Pyruvate, 2 mM L-glutamine. Transient transfection was performed using Lipofectamine 2000 followed by incubation for 48 h. siRNA against human NHA2 and control siRNA was purchased as siGENOME (Dharmacon, Lafayette, CO, USA) and the siRNA with the best knockdown (D-007345-04) was used. Cells were washed in cold PBS and lysed at 4 °C in lysis buffer (10 mM Tris·HCl, pH 7.8/150 mM NaCl/1 mM EDTA/1% Nonidet P-40) containing protease inhibitor mixture (Roche, Basel, Switzerland) and phosphatase inhibitors (Roche). Protein concentrations were equalized by quantitation and diluted in Laemmli sample buffer or incubated with primary antibody and protein G Plus Agarose beads (sc-2002; Santa Cruz Biotechnology) at 4 °C. Immunoprecipitates were washed and bound protein was eluted by boiling in Laemmli buffer. Ubiquitination assays were performed as described in detail using HA-tagged ubiquitin [59].

Mice

Mice always had free access to water and standard chow diet (#3432 from Provimi Kliba AG, Kaiseraugst, Switzerland) and were maintained on a 12 hours light/12 hours dark cycle. Generation of *Slc9b2*/NHA2 mice lacking exon 7 of the *NHA2* gene was described in detail previously [11]. NCC KO mice, originally generated by Schultheis et al. [35], were obtained from Prof. J. Loffing, University of Zürich, Switzerland. All mice used for experiments were littermates, males and completely backcrossed into C56BL/6J background (> 10 generations). Completeness of backcrossing was verified by microsatellite marker analysis, as described [10].

For urine collections, mice were housed in individual metabolic cages (Techniplast, Italy). Prior to collections, mice were allowed 2 days to adapt to the metabolic cages. Twenty-four hour urine samples were collected under mineral oil to avoid evaporation and with thymol as preservative. HCTZ was applied as a single intraperitoneal injection of vehicle (1:1 mixture of

0.9% NaCl solution with DMSO) or HCTZ (50 mg/kg; Sigma-Aldrich), and urine was collected for the next 6 hours.

Blood and urine analysis

Blood and urinary electrolytes, creatinine and urea were determined by the core laboratory of the University Hospital of Bern. Blood gas analysis was performed by an automated blood gas analyzer (ABL 800 FLEX, Radiometer Copenhagen, Denmark). Urine pH was measured using a pH microelectrode (Metrohm, Herisau, Switzerland). Urine ammonium was determined according to the Berthelot Protocol [60]. Urine osmolality was determined using a vapor pressure osmometer (VAPRO model 5600, Wescor South Logan, Utah, USA). Urinary aldosterone was determined by ^{125}I RIA (TKAL2 - Coat-A-Count Aldosterone kit, Siemens Healthcare Diagnostics, Germany), urinary catecholamines by ELISA (Catcombi ELISA, IBL International, Germany). Urinary glucocorticoids in mice were determined by gas chromatography-mass spectrometry (GC-MS) as described previously [61, 62].

Statistical analysis

For comparisons between groups the unpaired Student's t test (two groups) or 1-way ANOVA with Tukey post-hoc test (multiple groups) was used. Data were analyzed using GraphPad Prism 8.2 (GraphPad Software, San Diego, CA, USA). All statistical tests were two-sided and $p < 0.05$ was considered statistically significant. Unless stated otherwise, data are shown as means and error bars indicate SD.

Telemetry blood pressure profiles were analyzed with the statistical software SAS 9.4 on a X64 Windows workstation. Time series were seasonally adjusted, i.e. corrected for diurnal blood pressure variation. A general linear mixed effects model (GLIMMIX procedure) was used to estimate and compare the effects of diet and NHA2 and/or NCC KO, respectively, on blood pressure.

Study approval

All animal experiments were in accordance with the Swiss Animal Welfare Law and were approved by the local Veterinary Authority Bern (Veterinäramt Kanton Bern). Use of human kidney tissue was approved by the local Ethics Commission (Kantonale Ethikkomission Zürich).

Disclosures

DGF has served as a consultant for Otsuka Pharmaceuticals. DGF has received unrestricted research funding from Novartis, Abbvie and Otsuka Pharmaceuticals.

Acknowledgements

DGF was supported by the Swiss National Science Foundation (# grant 31003A_152829), the Swiss National Centre of Competence in Research (NCCR TransCure), the Novartis Research Foundation and by a Medical Research Position Award of the Foundation Prof. Dr. Max Cloëtta. We thank S. Uchida (constructs), C. Wagner and J. Loffing (antibodies), D. Ackermann (instructions on kidney perfusion), A. Vandewalle (mpkDCT$_4$ cells) and D. Firsov and G. Centeno for help with telemetry measurements and tubular microdissections.

SUPPLEMENTARY MATERIAL

1. Supplemental Figures 1-12

2. Supplemental Figure Legends

3. Supplemental Methods

Supplementary information is available on Kidney International's website.

References

1. Brett CL, Donowitz M, Rao R. Evolutionary origins of eukaryotic sodium/proton exchangers. *Am J Physiol Cell Physiol.* 2005;288:C223-239.
2. Fuster DG, Alexander RT. Traditional and emerging roles for the SLC9 Na+/H+ exchangers. *Pflugers Arch.* 2014;466:61-76.
3. Xiang M, Feng M, Muend S, et al. A human Na+/H+ antiporter sharing evolutionary origins with bacterial NhaA may be a candidate gene for essential hypertension. *Proc Natl Acad Sci U S A.* 2007;104:18677-18681.
4. Strazzullo P, Siani A, Cappuccio FP, et al. Red blood cell sodium-lithium countertransport and risk of future hypertension: the Olivetti Prospective Heart Study. *Hypertension.* 1998;31:1284-1289.
5. Laurenzi M, Cirillo M, Panarelli W, et al. Baseline sodium-lithium countertransport and 6-year incidence of hypertension. The Gubbio Population Study. *Circulation.* 1997;95:581-587.
6. Zerbini G, Mangili R, Gabellini D, et al. Modes of operation of an electroneutral Na+/Li+ countertransport in human skin fibroblasts. *Am J Physiol.* 1997;272:C1373-1379.
7. Cirillo M, Laurenzi M, Panarelli W, et al. Sodium-lithium countertransport and blood pressure change over time: the Gubbio study. *Hypertension.* 1996;27:1305-1311.
8. Canessa M, Adragna N, Solomon HS, et al. Increased sodium-lithium countertransport in red cells of patients with essential hypertension. *N Engl J Med.* 1980;302:772-776.
9. Mangili R, Bending JJ, Scott G, et al. Increased sodium-lithium countertransport activity in red cells of patients with insulin-dependent diabetes and nephropathy. *N Engl J Med.* 1988;318:146-150.
10. Deisl C, Anderegg M, Albano G, et al. Loss of Sodium/Hydrogen Exchanger NHA2 Exacerbates Obesity- and Aging-Induced Glucose Intolerance in Mice. *PLoS One.* 2016;11:e0163568.
11. Deisl C, Simonin A, Anderegg M, et al. Sodium/hydrogen exchanger NHA2 is critical for insulin secretion in beta-cells. *Proc Natl Acad Sci U S A.* 2013;110:10004-10009.
12. Liu HM, He JY, Zhang Q, et al. Improved detection of genetic loci in estimated glomerular filtration rate and type 2 diabetes using a pleiotropic cFDR method. *Mol Genet Genomics.* 2018;293:225-235.
13. Fuster DG, Zhang J, Shi M, et al. Characterization of the sodium/hydrogen exchanger NHA2. *J Am Soc Nephrol.* 2008;19:1547-1556.
14. Kondapalli KC, Todd Alexander R, Pluznick JL, et al. NHA2 is expressed in distal nephron and regulated by dietary sodium. *J Physiol Biochem.* 2017;73:199-205.
15. Hadchouel J, Ellison DH, Gamba G. Regulation of Renal Electrolyte Transport by WNK and SPAK-OSR1 Kinases. *Annu Rev Physiol.* 2016;78:367-389.
16. Castaneda-Bueno M, Arroyo JP, Zhang J, et al. Phosphorylation by PKC and PKA regulate the kinase activity and downstream signaling of WNK4. *Proc Natl Acad Sci U S A.* 2017;114:E879-E886.
17. Shibata S, Arroyo JP, Castaneda-Bueno M, et al. Angiotensin II signaling via protein kinase C phosphorylates Kelch-like 3, preventing WNK4 degradation. *Proc Natl Acad Sci U S A.* 2014;111:15556-15561.
18. Yoshizaki Y, Mori Y, Tsuzaki Y, et al. Impaired degradation of WNK by Akt and PKA phosphorylation of KLHL3. *Biochem Biophys Res Commun.* 2015;467:229-234.
19. Simon DB, Nelson-Williams C, Bia MJ, et al. Gitelman's variant of Bartter's syndrome, inherited hypokalaemic alkalosis, is caused by mutations in the thiazide-sensitive Na-Cl cotransporter. *Nat Genet.* 1996;12:24-30.

20. Gitelman HJ, Graham JB, Welt LG. A new familial disorder characterized by hypokalemia and hypomagnesemia. *Trans Assoc Am Physicians.* 1966;79:221-235.
21. Wilson FH, Disse-Nicodeme S, Choate KA, et al. Human hypertension caused by mutations in WNK kinases. *Science.* 2001;293:1107-1112.
22. Boyden LM, Choi M, Choate KA, et al. Mutations in kelch-like 3 and cullin 3 cause hypertension and electrolyte abnormalities. *Nature.* 2012;482:98-102.
23. Louis-Dit-Picard H, Barc J, Trujillano D, et al. KLHL3 mutations cause familial hyperkalemic hypertension by impairing ion transport in the distal nephron. *Nat Genet.* 2012;44:456-460, S451-453.
24. Mayan H, Vered I, Mouallem M, et al. Pseudohypoaldosteronism type II: marked sensitivity to thiazides, hypercalciuria, normomagnesemia, and low bone mineral density. *J Clin Endocrinol Metab.* 2002;87:3248-3254.
25. Loffing J, Loffing-Cueni D, Valderrabano V, et al. Distribution of transcellular calcium and sodium transport pathways along mouse distal nephron. *Am J Physiol Renal Physiol.* 2001;281:F1021-1027.
26. Van Vliet BN, McGuire J, Chafe L, et al. Phenotyping the level of blood pressure by telemetry in mice. *Clin Exp Pharmacol Physiol.* 2006;33:1007-1015.
27. McCormick JA, Mutig K, Nelson JH, et al. A SPAK isoform switch modulates renal salt transport and blood pressure. *Cell Metab.* 2011;14:352-364.
28. Pacheco-Alvarez D, Cristobal PS, Meade P, et al. The Na+:Cl- cotransporter is activated and phosphorylated at the amino-terminal domain upon intracellular chloride depletion. *J Biol Chem.* 2006;281:28755-28763.
29. Richardson C, Rafiqi FH, Karlsson HK, et al. Activation of the thiazide-sensitive Na+-Cl- cotransporter by the WNK-regulated kinases SPAK and OSR1. *J Cell Sci.* 2008;121:675-684.
30. Yang SS, Morimoto T, Rai T, et al. Molecular pathogenesis of pseudohypoaldosteronism type II: generation and analysis of a Wnk4(D561A/+) knockin mouse model. *Cell Metab.* 2007;5:331-344.
31. Gamba G. Regulation of the renal Na+-Cl- cotransporter by phosphorylation and ubiquitylation. *Am J Physiol Renal Physiol.* 2012;303:F1573-1583.
32. Kocinsky HS, Girardi AC, Biemesderfer D, et al. Use of phospho-specific antibodies to determine the phosphorylation of endogenous Na+/H+ exchanger NHE3 at PKA consensus sites. *Am J Physiol Renal Physiol.* 2005;289:F249-258.
33. Kocinsky HS, Dynia DW, Wang T, et al. NHE3 phosphorylation at serines 552 and 605 does not directly affect NHE3 activity. *Am J Physiol Renal Physiol.* 2007;293:F212-218.
34. Lytle C, Forbush B, 3rd. The Na-K-Cl cotransport protein of shark rectal gland. II. Regulation by direct phosphorylation. *J Biol Chem.* 1992;267:25438-25443.
35. Schultheis PJ, Lorenz JN, Meneton P, et al. Phenotype resembling Gitelman's syndrome in mice lacking the apical Na+-Cl- cotransporter of the distal convoluted tubule. *J Biol Chem.* 1998;273:29150-29155.
36. Loffing J, Vallon V, Loffing-Cueni D, et al. Altered renal distal tubule structure and renal Na(+) and Ca(2+) handling in a mouse model for Gitelman's syndrome. *J Am Soc Nephrol.* 2004;15:2276-2288.
37. Becker M, Nothwang HG, Friauf E. Differential expression pattern of chloride transporters NCC, NKCC2, KCC1, KCC3, KCC4, and AE3 in the developing rat auditory brainstem. *Cell Tissue Res.* 2003;312:155-165.
38. Peng KC, Cluzeaud F, Bens M, et al. Tissue and cell distribution of the multidrug resistance-associated protein (MRP) in mouse intestine and kidney. *J Histochem Cytochem.* 1999;47:757-768.

39. Duong Van Huyen JP, Bens M, Teulon J, et al. Vasopressin-stimulated chloride transport in transimmortalized mouse cell lines derived from the distal convoluted tubule and cortical and inner medullary collecting ducts. *Nephrol Dial Transplant.* 2001;16:238-245.
40. San-Cristobal P, Pacheco-Alvarez D, Richardson C, et al. Angiotensin II signaling increases activity of the renal Na-Cl cotransporter through a WNK4-SPAK-dependent pathway. *Proc Natl Acad Sci U S A.* 2009;106:4384-4389.
41. Talati G, Ohta A, Rai T, et al. Effect of angiotensin II on the WNK-OSR1/SPAK-NCC phosphorylation cascade in cultured mpkDCT cells and in vivo mouse kidney. *Biochem Biophys Res Commun.* 2010;393:844-848.
42. Shibata S, Zhang J, Puthumana J, et al. Kelch-like 3 and Cullin 3 regulate electrolyte homeostasis via ubiquitination and degradation of WNK4. *Proc Natl Acad Sci U S A.* 2013;110:7838-7843.
43. Ishizawa K, Wang Q, Li J, et al. Calcineurin dephosphorylates Kelch-like 3, reversing phosphorylation by angiotensin II and regulating renal electrolyte handling. *Proc Natl Acad Sci U S A.* 2019;116:3155-3160.
44. Hofstetter W, Siegrist M, Simonin A, et al. Sodium/hydrogen exchanger NHA2 in osteoclasts: subcellular localization and role in vitro and in vivo. *Bone.* 2010;47:331-340.
45. Ramseyer VD, Ortiz PA, Carretero OA, et al. Angiotensin II-mediated hypertension impairs nitric oxide-induced NKCC2 inhibition in thick ascending limbs. *Am J Physiol Renal Physiol.* 2016;310:F748-F754.
46. Krug AW, Papavassiliou F, Hopfer U, et al. Aldosterone stimulates surface expression of NHE3 in renal proximal brush borders. *Pflugers Arch.* 2003;446:492-496.
47. Crajoinas RO, Polidoro JZ, Carneiro de Morais CP, et al. Angiotensin II counteracts the effects of cAMP/PKA on NHE3 activity and phosphorylation in proximal tubule cells. *Am J Physiol Cell Physiol.* 2016;311:C768-C776.
48. Nijenhuis T, Vallon V, van der Kemp AW, et al. Enhanced passive Ca2+ reabsorption and reduced Mg2+ channel abundance explains thiazide-induced hypocalciuria and hypomagnesemia. *J Clin Invest.* 2005;115:1651-1658.
49. Uzdavinys P, Coincon M, Nji E, et al. Dissecting the proton transport pathway in electrogenic Na+/H+ antiporters. *Proc Natl Acad Sci U S A.* 2017;114:E1101-E1110.
50. Chintapalli VR, Kato A, Henderson L, et al. Transport proteins NHA1 and NHA2 are essential for survival, but have distinct transport modalities. *Proc Natl Acad Sci U S A.* 2015;112:11720-11725.
51. Lippiat JD, Smith AJ. The CLC-5 2Cl(-)/H(+) exchange transporter in endosomal function and Dent's disease. *Front Physiol.* 2012;3:449.
52. Wakabayashi M, Mori T, Isobe K, et al. Impaired KLHL3-mediated ubiquitination of WNK4 causes human hypertension. *Cell Rep.* 2013;3:858-868.
53. Sasaki E, Susa K, Mori T, et al. KLHL3 Knockout Mice Reveal the Physiological Role of KLHL3 and the Pathophysiology of Pseudohypoaldosteronism Type II Caused by Mutant KLHL3. *Mol Cell Biol.* 2017;37.
54. Treier M, Staszewski LM, Bohmann D. Ubiquitin-dependent c-Jun degradation in vivo is mediated by the delta domain. *Cell.* 1994;78:787-798.
55. Bens M, Vallet V, Cluzeaud F, et al. Corticosteroid-dependent sodium transport in a novel immortalized mouse collecting duct principal cell line. *J Am Soc Nephrol.* 1999;10:923-934.
56. Diepens RJ, den Dekker E, Bens M, et al. Characterization of a murine renal distal convoluted tubule cell line for the study of transcellular calcium transport. *Am J Physiol Renal Physiol.* 2004;286:F483-489.

57. Duong Van Huyen J, Bens M, Vandewalle A. Differential effects of aldosterone and vasopressin on chloride fluxes in transimmortalized mouse cortical collecting duct cells. *J Membr Biol.* 1998;164:79-90.
58. Battaglino RA, Pham L, Morse LR, et al. NHA-oc/NHA2: a mitochondrial cation-proton antiporter selectively expressed in osteoclasts. *Bone.* 2008;42:180-192.
59. Simonin A, Fuster D. Nedd4-1 and beta-arrestin-1 are key regulators of Na+/H+ exchanger 1 ubiquitylation, endocytosis, and function. *J Biol Chem.* 2010;285:38293-38303.
60. Stehberger PA, Shmukler BE, Stuart-Tilley AK, et al. Distal renal tubular acidosis in mice lacking the AE1 (band3) Cl-/HCO3- exchanger (slc4a1). *J Am Soc Nephrol.* 2007;18:1408-1418.
61. Quattropani C, Vogt B, Odermatt A, et al. Reduced activity of 11 beta-hydroxysteroid dehydrogenase in patients with cholestasis. *J Clin Invest.* 2001;108:1299-1305.
62. Vogt B, Dick B, N'Gankam V, et al. Reduced 11beta-hydroxysteroid dehydrogenase activity in patients with the nephrotic syndrome. *J Clin Endocrinol Metab.* 1999;84:811-814.

FIGURES

Figure 1. NHA2 localizes to DCT in murine kidney. A) Murine kidney cryosections of WT (left panel) or NHA2 KO mice (right panel) stained with NHA2 antibody. Middle panel: WT kidney stained with secondary antibody only. Scale bars: 100 µm. B) Murine WT kidney cryosections stained with antibodies for NHA2 and parvalbumin (a marker of DCT1) or TRPV5 (a marker of DCT2 and CNT, respectively). Scale bars: 50 µm. C) NHA2 mRNA expression in microdissected tubular segments, quantified by real-time PCR and normalized to GAPDH. Each dot represents a microdissection from a separate mouse. PCT proximal convoluted tubule; PST proximal straight tubule; TAL thick ascending limb of Henle; DCT distal convoluted tubule; CNT connecting tubule; CCD cortical collecting duct. Asterisk denotes significance for comparison to all other segments (ANOVA with Tukey post-hoc test; ***$p < 0.01$).

Figure 2. Blood pressure is reduced in NHA2 KO mice. Mean arterial pressure measured by telemetry under normal (0.2 %; NS), low (<0.03%; LS) and high Na^+ (8 %; HS) diets in WT and NHA2 KO mice. N=6-9 mice/genotype and condition. Asterisks denote significance for the indicated comparisons (analyzed by general linear mixed effects model; ***$p < 0.001$).

Figure 3. WNK-SPAK-NCC axis is attenuated in NHA2 KO mice. A) Immunoblots of kidney tissue lysates harvested from WT and NHA2 KO mice using indicated primary antibodies. Tubulin served as a loading control. Each lane identifies results from a separate mouse. B) Dot-plot graphs show the results of quantification. Asterisks denote significance for the indicated comparison (unpaired t-test; *$p < 0.05$, **$p < 0.01$, ***$p < 0.001$). C)

Urinary sodium (Na) and D) calcium (Ca) excretion in response to application of hydrochlorothiazide (HCTZ; 50 mg/kg i.p.) or vehicle in WT and NHA2 KO mice. Asterisks denote significance for the indicated comparisons (ANOVA with Tukey post-hoc test; *p <0.05, **p < 0.01, NS=not significant).

Figure 4. Loss of NCC abolishes blood pressure and calciuria phenotype in NHA2 KO mice. A) Mean arterial pressure measured by telemetry under normal (0.2 %; NS), low (<0.03%; LS) and high Na+ (8 %; HS) diets in NCC KO and NCC NHA2 double KO mice. N=6-8 mice/genotype and condition. Asterisks denote significance for the indicated comparison (analyzed by general linear mixed effects model; ***p < 0.001, NS = not significant). B) Urinary calcium (Ca) excretion normalized to creatinine in WT, NHA2 KO, NCC KO and NCC/NHA2 double KO mice. Asterisks denote significance for the indicated comparisons (ANOVA with Tukey post-hoc test; ***p < 0.001, NS=not significant).

Figure 5. Knock-down of NHA2 reduces WNK4 expression and NCC phosphorylation in mpkDCT4. A) Immunoblot of lysates from mpkDCT4 cells treated with control or NHA2 targeting siRNA. B) Quantification of endogenous WNK4 expression (unpaired t-test; ***p < 0.001). C, E) Immunoblot of lysates from mpkDCT4-cells treated with control or NHA2-targetting siRNA, stimulated for 30 minutes with basic or low chloride media (C) or for 60 minutes with either vehicle or 10^{-6} M of Angiotensin II (E). D, F) Quantification of endogenous NCC phosphorylation at position T53. Immunoblots show biological replicates. Asterisks denote significance for the indicated comparisons (ANOVA with Tukey post-hoc test; *p < 0.05, **p < 0.01, ***p < 0.001, NS=not significant).

Figure 6. NHA2 depletion causes increased ubiquitylation and proteasomal degradation of WNK4 via a KLHL3-dependent mechanism. A) Representative immunoblots of lysates from HEK293 cells transfected with WNK4-FLAG and ubiquitin-HA and either control or NHA2 targeting siRNA. B) Quantification of WNK4 expression and WNK4 ubiquitylation. C) Immunoblot of lysates from HEK293 cells transfected with WNK4-FLAG and either control or NHA2 targeting siRNA. Before lysis, cells were treated for 3h with vehicle (DMSO) or 20μM MG132. D) Quantification of WNK4 expression. E) Immunoblot of lysates from HEK293 cells transfected with wild-type WNK4 or indicated WNK mutants. F) Quantification of WNK4 expression. Immunoblots show biological replicates. Asterisks denote significance for the indicated comparisons (unpaired t-test 6B, ANOVA with Tukey post-hoc test 6D and 6F; *$p < 0.05$, **$p < 0.01$, NS=not significant).

Figure 7. NHA2 knock-down causes a blunted response to PKA- and PKC-mediated increase of WNK4 expression. A) Representative immunoblots and corresponding quantifications (B) of immunoprecipitated KLHL3-GFP from HEK293 cells treated with control or NHA2-targetting siRNA, cotransfected with KLHL3-GFP. Cells were starved for 1 h and then treated for 1 h with vehicle, the PKC activator TPA (200 nM), the PKC inhibitor BIM (4 μM), or a combination of both. Samples were blotted with KLHL3 and phospho-PKC substrate (R/KXS^P) antibodies, respectively. C), E), G), I) Representative immunoblots and corresponding quantifications (D, F, H, J) of lysates from HEK293 cells treated with control or NHA2-targeting siRNA and cotransfected with WNK4-FLAG and KLHL3-GFP. Before lysis, cells were treated for 1h with vehicle, the PKC activator TPA (200 nM) or the PKA activator Forskolin (FK; 30 μM), respectively. C), E) were blotted with monoclonal FLAG-antibody and G) with phospho-PKA substrate ($RRXS^P/T^P$) or I) phospho-PKC substrate (R/KXS^P) antibody, respectively. Immunoblots show biological replicates. Asterisks denote

significance for the indicated comparisons (ANOVA with Tukey post-hoc test; **$p < 0.01$, ***$p < 0.001$, NS=not significant).

TABLES

Table 1. Blood parameters of WT and NHA2 KO mice

Parameter	**WT**	**NHA2 KO**	
Na (mM)	148.5±2.14	150.2±1.58	NS
K (mM)	4.22±0.41	4.36±0.61	NS
Cl (mM)	114.2±2.50	114.90±3.41	NS
Ca (mM)	2.20±0.09	2.19±0.09	NS
Ca ion. (mM)	1.24±0.03	1.25±0.06	NS
P (mM)	2.94±0.71	2.78±0.59	NS
Mg (mM)	1.08±0.11	1.09±0.10	NS
Creatinine (µM)	13.8±2.20	13.5±2.28	NS
Urea (mM)	7.64±2.07	8.55±2.85	NS
Uric acid (µM)	79.2±17.56	77.16±28.08	NS
pH	7.33±0.06	7.33±0.04	NS
pCO_2 (mmHg)	47.65±15.02	49.23±13.55	NS
HCO_3 (mM)	24.57±4.12	25.18±4.70	NS
PTH (pg/ml)	155.6±71.3	137.4±61.1	NS
$1,25(OH)_2$ Vitamin D_3 (pmol/l)	403.8±73.3	391.1±88.9	NS

N = 12 per genotype. Results shown are mean ± SD. Unpaired t-test; NS= not significant.

Average body weight of mice studied: WT 24±1.6 g and NHA2 KO 23.9±1.3 g, NS.

Table 2. Urine parameters of WT and NHA2 KO mice

Parameter	**WT**	**NHA2 KO**	
pH	6.16±0.23	6.32±0.24	NS
Volume (µl / 24 h)	1535±364	1430±586	NS
Osmolality (mosm / kg H_20)	2545±923	2801±986	NS
Creatinine (µmol / 24 h)	3.97±0.68	3.30±0.84	NS
Urea (mmol / 24 h)	2.20±0.42	1.51±0.50	NS
Na (mM) / Creat (mM)	51.03±7.38	54.04±11.55	NS
K (mM) / Creat (mM)	125.61±13.44	136.89±22.97	NS
Cl (mM) / Creat (mM)	101.71±22.38	104.76±12.66	NS
Ca (mM) / Creat (mM)	1.09±0.3	0.66±0.23	***
P (mM) / Creat (mM)	36.25±8.73	43.06±10.79	NS
Mg (mM) / Creat (mM)	10.01±0.89	10.34±1.05	NS
NH_4 (mM) / Creat (mM)	17.47±8.73	19.90±5.70	NS
Aldosterone (pg) / Creat (µM)	895.04±394.08	1163.39±390.96	*
Corticosterone (ng) / Creat (µM)	34.68±13.02	37.82±18.56	NS
Adrenaline (ng) / Creat (µM)	4.16±1.37	5.70±2.76	NS
Noradrenaline (ng) / Creat (µM)	52.30±12.4	57.52±27.92	NS

N = 12 per genotype. Results shown are mean ± SD. Unpaired t-test; *$p < 0.05$, ***$p < 0.001$, NS=not significant.

Average body weight of mice studied: WT 24±1.6 g and NHA2 KO 23.9±1.3 g, NS.